Supporting Information

N-doped Engineering on High-Voltage $LiNi_{0.5}Mn_{1.5}O_4$ Cathode with Superior Cycling Capability for Wide Temperature Lithium-Ion Batteries

Mingzhu Li[a], Qingping Li[a], Maofeng Hu[a], Yongxu Du[a], Zhipeng Duan[a], Hongguang Fan[a], Yongpeng Cui[b], Shuang Liu[a], Yongcheng Jin[a], Wei Liu[a]**

[a]School of Materials Science and Engineering, Ocean University of China, Qingdao 266100, People's Republic of China.

[b]School of Materials Science and Engineering, China University of Petroleum, Qingdao 266580, People's Republic of China.

**Corresponding Author E-mail: weiliu@ouc.edu.cn. jinyongcheng@ouc.edu.cn*

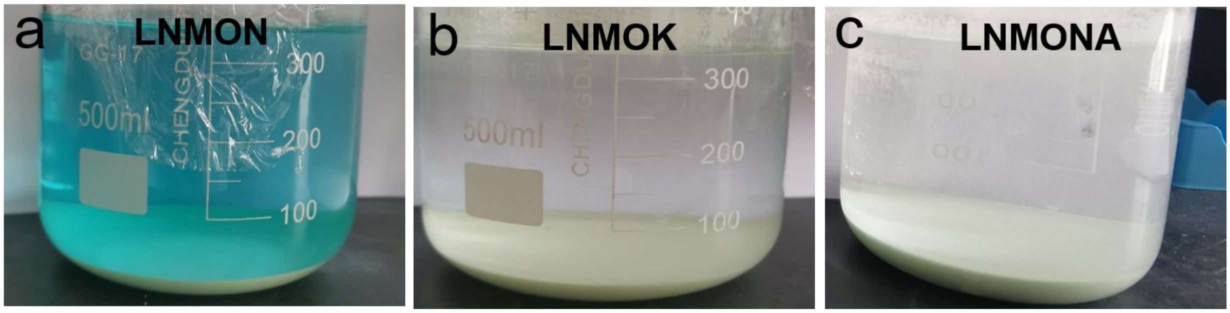

Figure S1. The color of supernatant changed after adding different precipitators during co-precipitation.

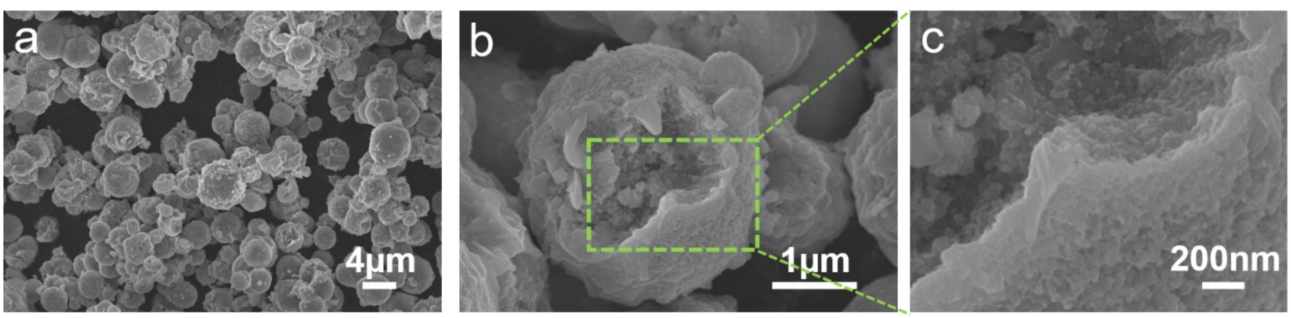

Figure S2. SEM images of the prepared LNMOK.

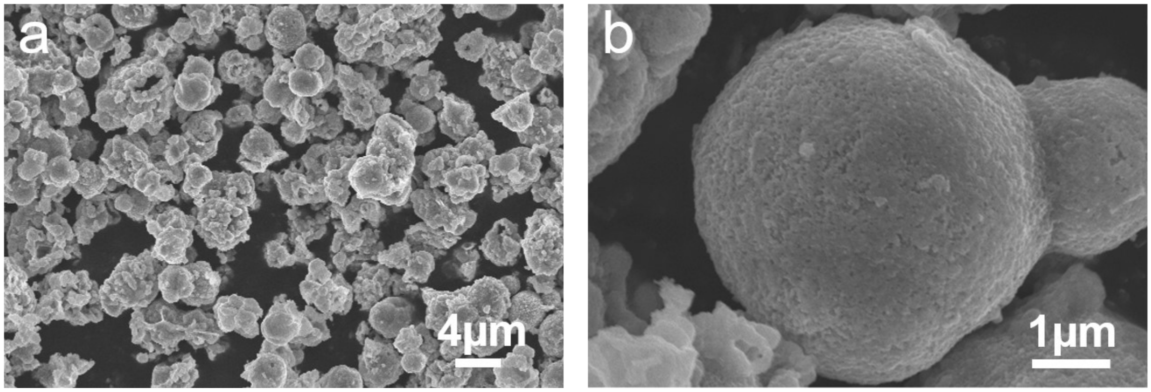

Figure S3. SEM images of the prepared LNMONA.

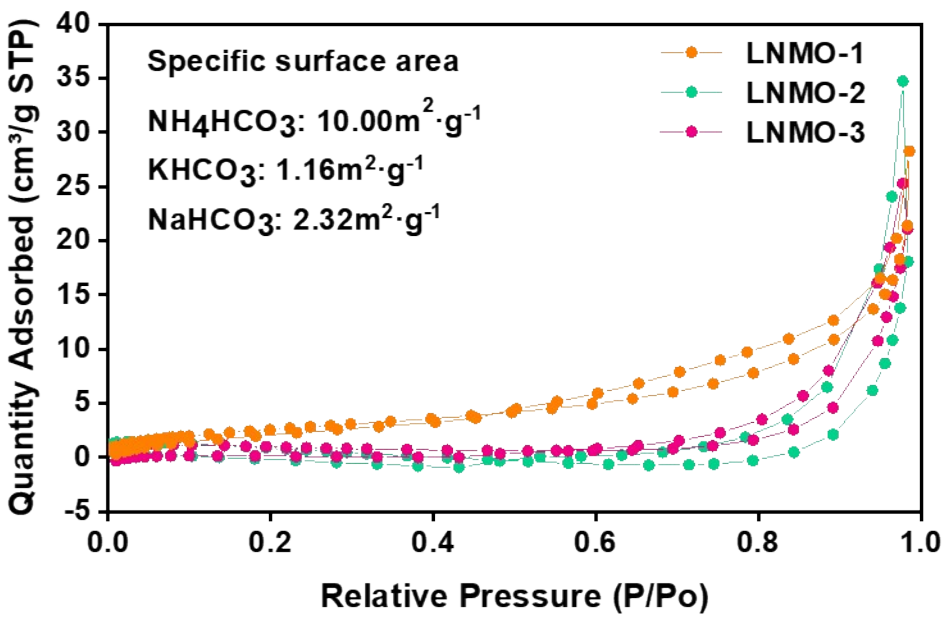

Figure S4. Nitrogen adsorption-desorption isotherms of all LNMO samples.

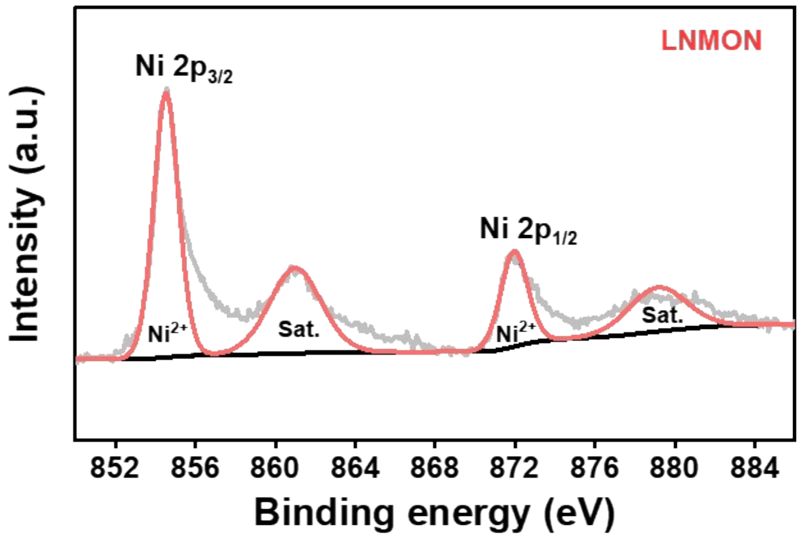

Figure S5. XPS spectra of Ni 2p for LNMON sample.

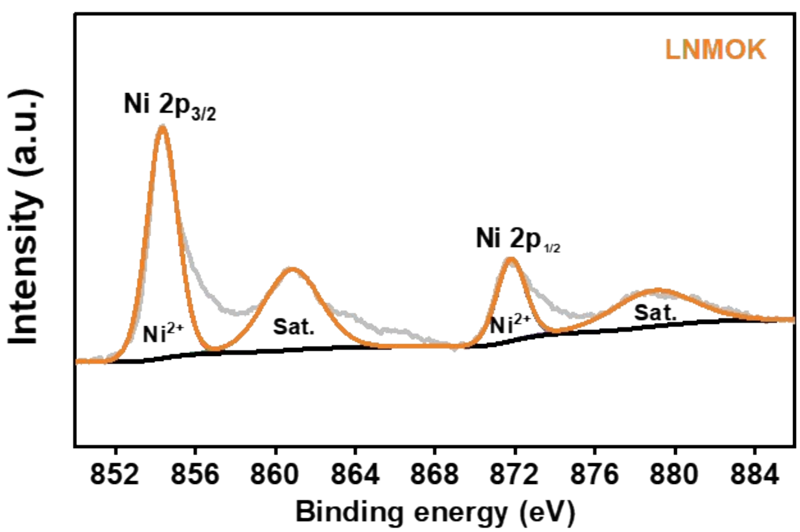

Figure S6. XPS spectra of Ni 2p for LNMOK sample.

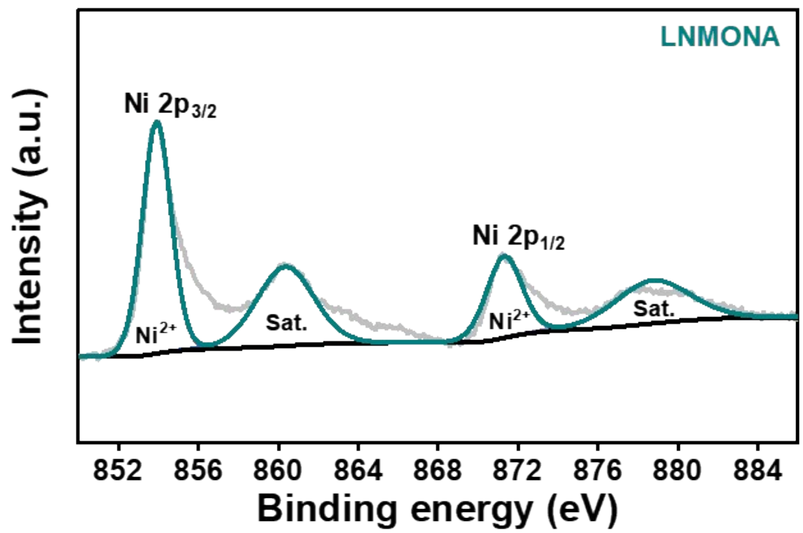

Figure S7. XPS spectra of Ni 2p for LNMONA sample.

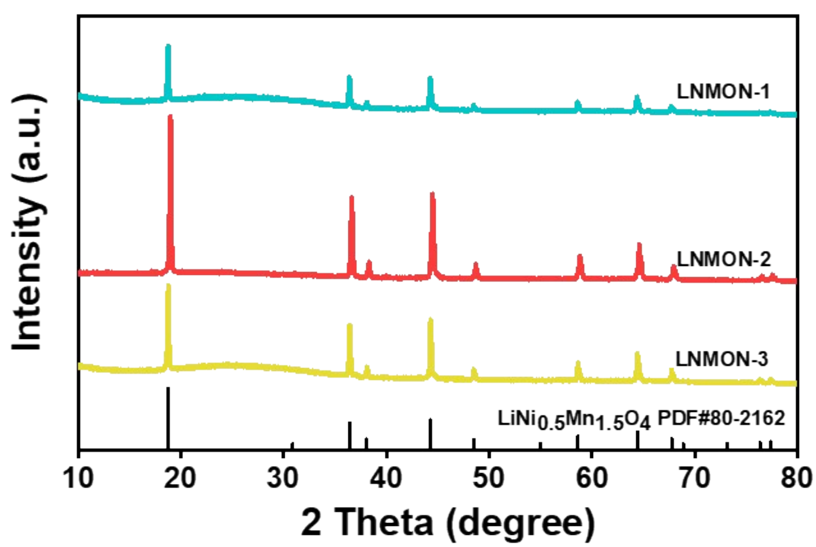

Figure S8. XRD patterns of LNMONs.

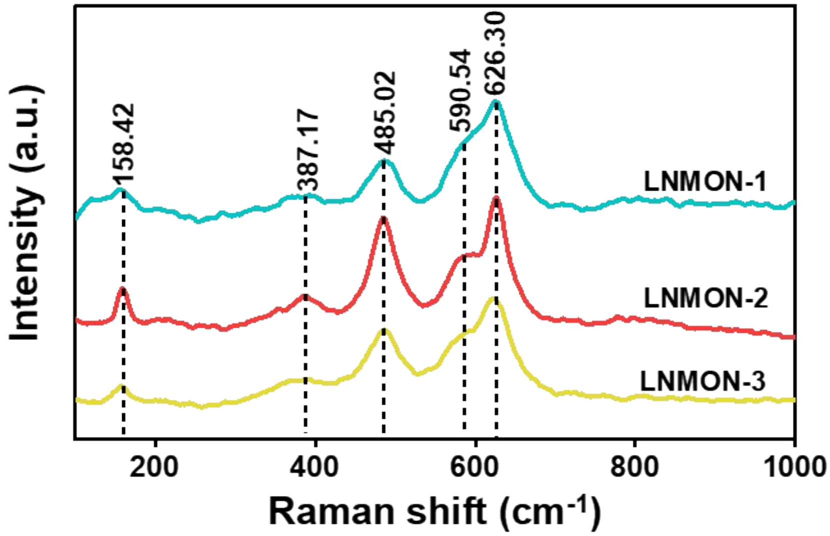

Figure S9. Raman spectroscopy of LNMONs.

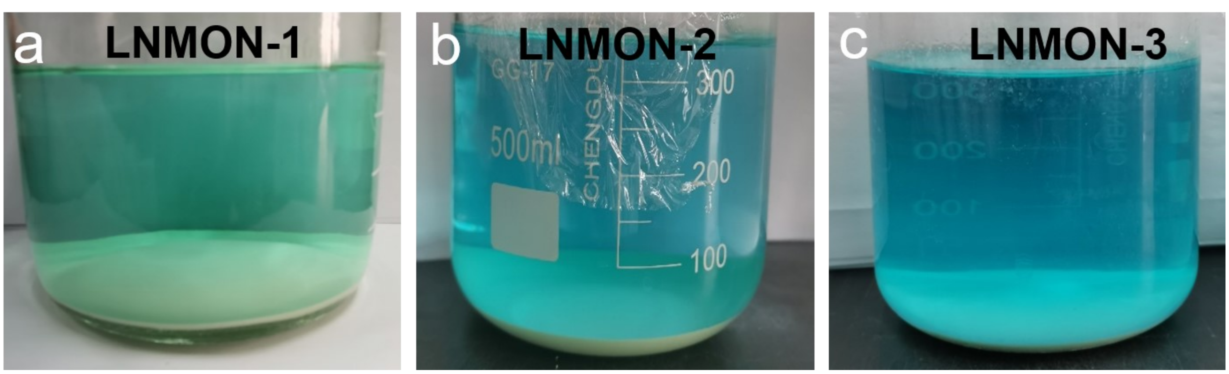

Figure S10. Color of carbonate precursors of LNMONs with different nitrogen content.

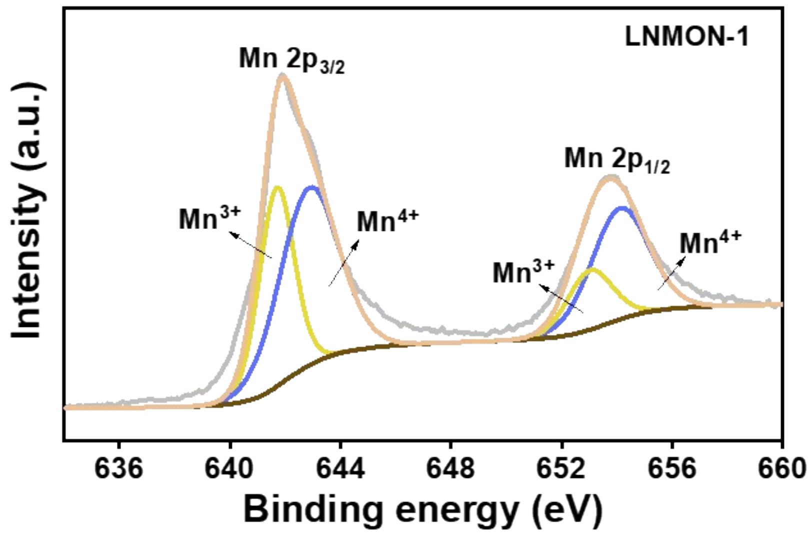

Figure S11. XPS spectra of Mn 2p for LNMON-1 sample.

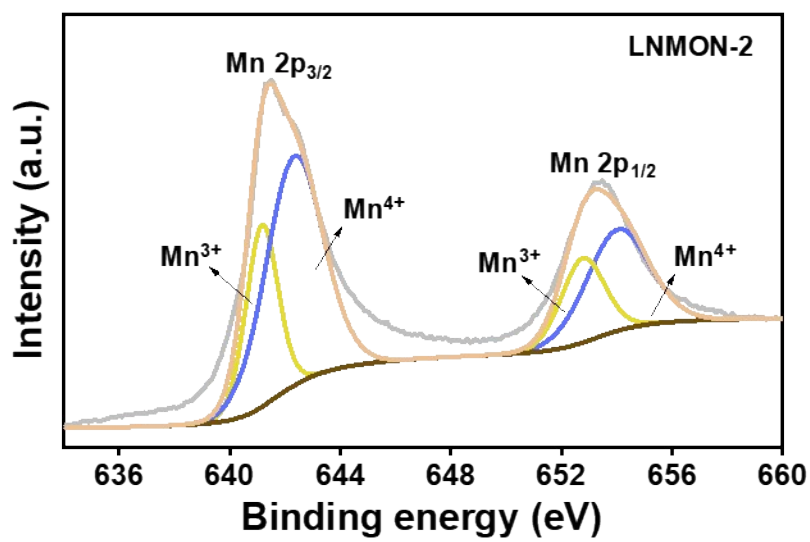

Figure S12. XPS spectra of Mn 2p for LNMON-2 sample.

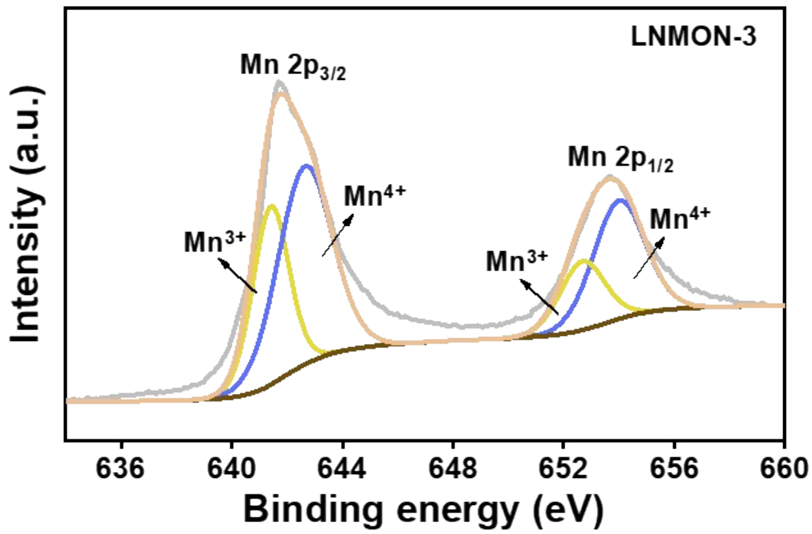

Figure S13. XPS spectra of Mn 2p for LNMON-3 sample.

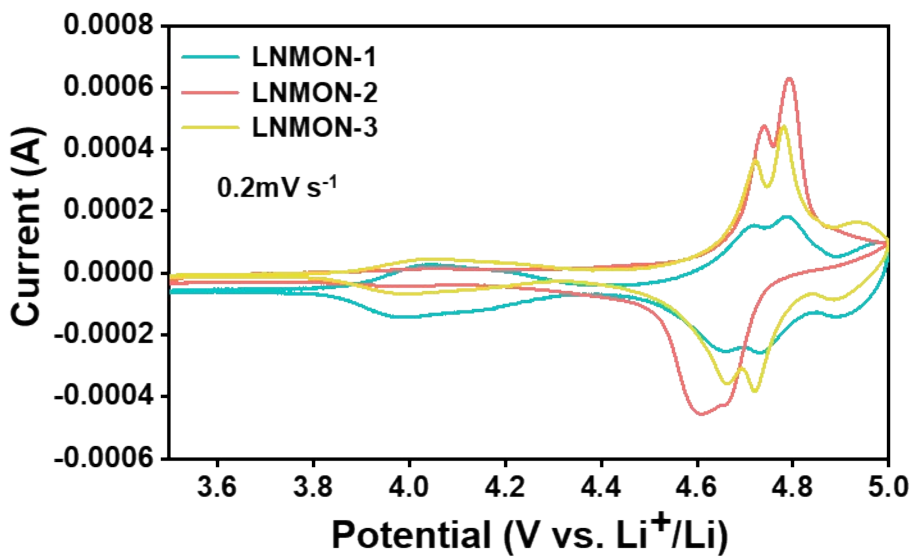

Figure S14. CV curves of all LNMON (1-3) samples scanned at 0.2 mV s^{-1} from 3.5 V to 5.0 V voltage window.

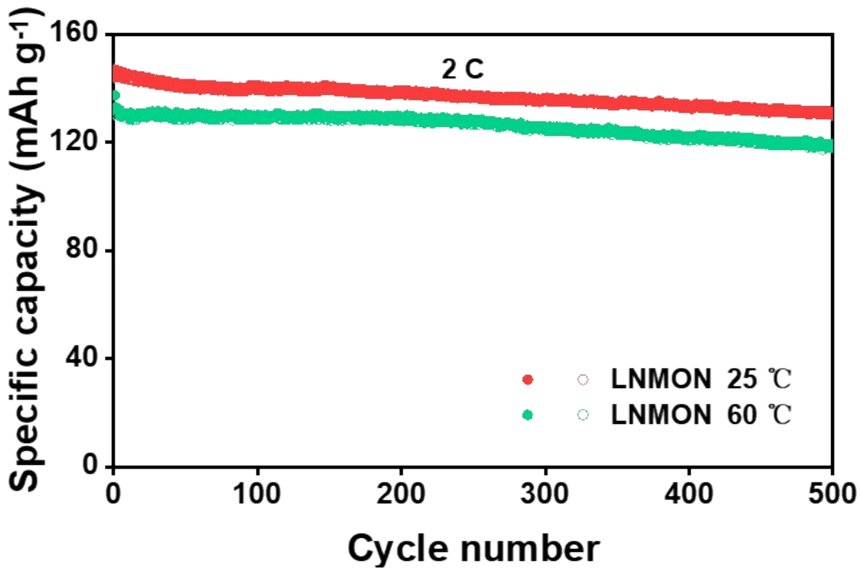

Figure S15. Electrochemical performance of LNMON at 500 cycles at 2C current density at different temperatures.

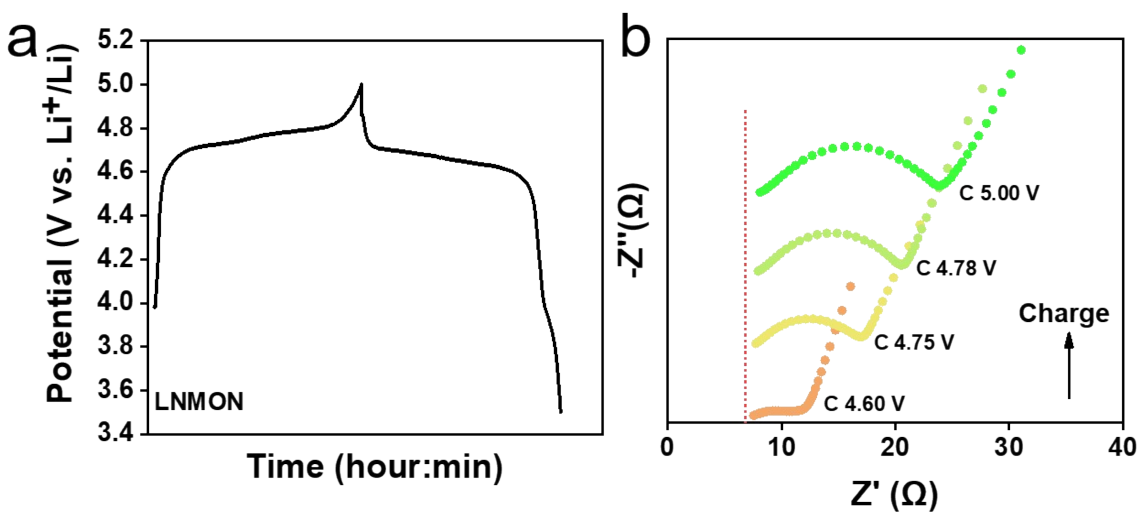

Figure S16. (a) Charge and discharge curves of LNMON. (b) Impedance of LNMON at different voltages during charging.

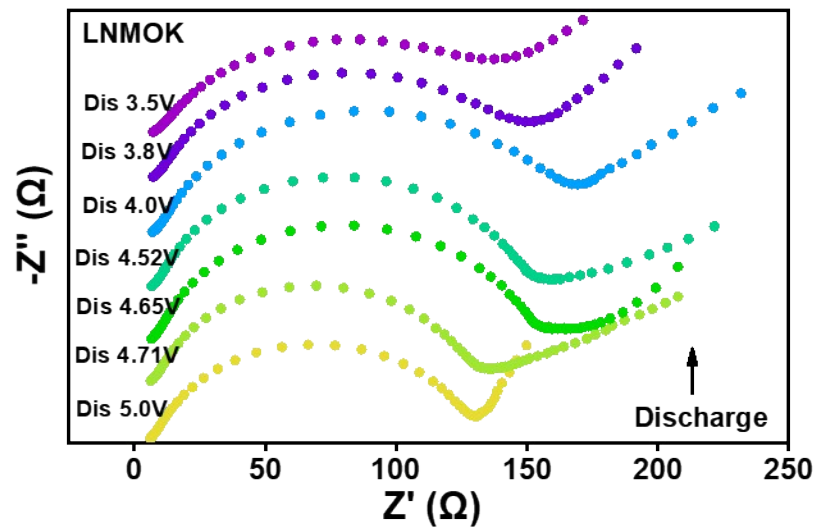

Figure S17. Impedance of LNMOK at different voltages during discharge.

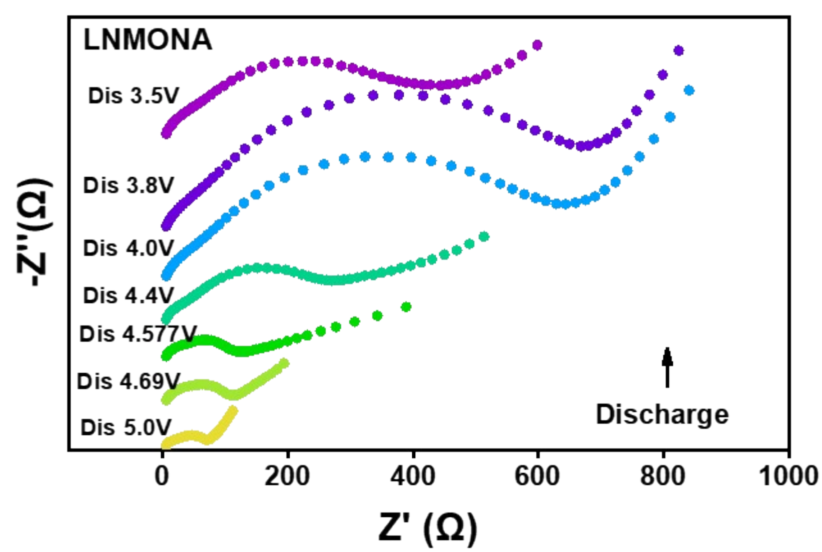

Figure S18. Impedance of LNMONA at different voltages during discharge.

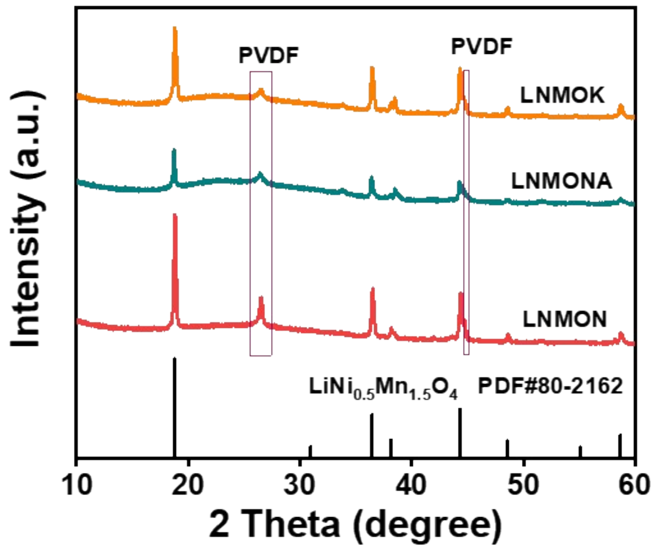

Figure S19. XRD of all samples after 500 cycles at 2 C.

Table S1. Comparisons of the cycling performance of LNMON electrode with other LNMO-based anode materials in LIBs reported in open literature.

Sample	Cycling performance	Ref.
$LiNi_{0.45}Cr_{0.1}Mn_{1.45}O_4$	106.7 mAh g^{-1} (1000 cycles, 1 C at 25 °C, capacity retention is 82.75 %)	1.
LiNi0.50Mn1.49Mg0.01O3.97F0.03	130 mAh g^{-1} (200 cycles, 1 C, capacity retention is 90.9 %)	2.
2 wt% Li2ZrO3-coated LNMO	101.6 mAh g^{-1} (1000 cycles, 5 C at 25 °C, capacity retention is 82.4 %)	3

LNMO Co-700	118 mAh g^{-1} (500 cycles, 1 C at 25 ℃, capacity retention is 93 %)	4
Sb002-LNMO	105.4 mAh g^{-1} (3000 cycles, 1 C, capacity retention is 72.4 %)	Ref. 27 in the text
Mg0.1-LNMO	103.4 mAh g^{-1} (2200 cycles, 10 C, capacity retention is 87.3 %)	Ref. 28 in the text
CoTi-LNMO	100.86 mAh g^{-1} (900 cycles, 1 C at 25 ℃, capacity retention is 82 %)	Ref. 29 in the text
LNMZO-0.005	123.8 mAh g^{-1} (200 cycles, 1 C, capacity retention is 93.93 %)	Ref. 30 in the text
LNMON	**112 mAh g^{-1} (3000 cycles, 10 C at 25 ℃, capacity retention is 92.49 %)**	**This work**

Table S2. The diffusion coefficient of lithium ion is calculated by CV curve at different peak position ($\times 10^{-10}$ cm^2 s^{-1}).

Sample	O1	O2	R	D_a[a)]
LNMON	0.29	0.66	0.49	0.48
LNMOK	0.18	0.39	0.34	0.30
LNMONA	0.14	0.29	0.21	0.21

[a] Da represents the average diffusion coefficient of each group of samples.

Table S3. Results of fitting different impedance values of LNMOs (Ω).

Sample	Rs	Rct (before cycle)	Rct (after cycle)
LNMON	3.16	12.51	82.36
LNMOK	4.16	15.27	88.00
LNMONA	3.02	20.68	98.08

References

1. J. Wang, P. Nie, G. Xu, J. Jiang, Y. Wu, R. Fu, H. Dou and X. Zhang, *Adv. Funct. Mater.*, 2018, **28**, 1704808.
2. A. Wei, W. Li, Q. Chang, X. Bai, R. He, L. Zhang, Z. Liu and Y. Wang, *Electrochim. Acta*, 2019, **323**, 134692.
3. J. Zhang, G. Sun, Y. Han, F. Yu, X. Qin, G. Shao and Z. Wang, *Electrochim. Acta*, 2020, **343**, 136105.
4. Y. Xue, L.-L. Zheng, J. Wang, J.-G. Zhou, F.-D. Yu, G.-J. Zhou and Z.-B. Wang, *ACS Appl. Energy Mater.*, 2019, **2**, 2982-2989.